Cancer Cell
Article

Functional Interaction of Plasmacytoid Dendritic Cells with Multiple Myeloma Cells: A Therapeutic Target

Dharminder Chauhan,[1,5,*] Ajita V. Singh,[1,5] Mohan Brahmandam,[1] Ruben Carrasco,[1] Madhavi Bandi,[1] Teru Hideshima,[1] Giada Bianchi,[1] Klaus Podar,[1] Yu-Tzu Tai,[1] Constantine Mitsiades,[1] Noopur Raje,[1] David L. Jaye,[2] Shaji K. Kumar,[3] Paul Richardson,[1] Nikhil Munshi,[4] and Kenneth C. Anderson[1,*]

[1]The LeBow Institute for Myeloma Therapeutics and Jerome Lipper Center for Myeloma Research, Department of Medical Oncology, Dana-Farber Cancer Institute, Harvard Medical School, Boston, MA 02115, USA
[2]Department of Pathology and Laboratory Medicine, Emory University, Atlanta, GA 30322, USA
[3]Department of Hematology, Mayo Clinic, Rochester, MN 55905, USA
[4]Veterans Administration Boston Healthcare System, Harvard Medical School, Boston, MA 02115, USA
[5]These authors contributed equally to this work
*Correspondence: kenneth_anderson@dfci.harvard.edu (K.C.A.), dharminder_chauhan@dfci.harvard.edu (D.C.)
DOI 10.1016/j.ccr.2009.08.019

SUMMARY

Multiple myeloma (MM) remains incurable despite novel therapies, suggesting the need for further identification of factors mediating tumorigenesis and drug resistance. Using both in vitro and in vivo MM xenograft models, we show that plasmacytoid dendritic cells (pDCs) in the bone marrow (BM) microenvironment both mediate immune deficiency characteristic of MM and promote MM cell growth, survival, and drug resistance. Microarray, cell signaling, cytokine profile, and immunohistochemical analysis delineate the mechanisms mediating these sequelae. Although pDCs are resistant to novel therapies, targeting Toll-like receptors with CpG oligodeoxynucleotides both restores pDC immune function and abrogates pDC-induced MM cell growth. Our study therefore validates targeting pDC-MM interactions as a therapeutic strategy to overcome drug resistance in MM.

INTRODUCTION

Multiple myeloma (MM) is diagnosed in 15,000 new individuals annually. The median survival has been prolonged from 3–4 to 7 years, especially in patients younger than age 50 (Brenner et al., 2008; Kumar et al., 2008). However, despite important advances, such as the biological agents bortezomib, thalidomide, and lenalidomide, MM remains incurable due to the development of drug resistance, which manifests as relapsed/refractory disease (Anderson, 2007). The molecular mechanisms whereby MM cells evade drug-induced cytotoxicity and acquire drug-resistant phenotypes include interaction of MM cells with their bone marrow (BM) microenvironment (Dalton and Anderson, 2006; Hideshima et al., 2007). The BM milieu contains stromal cells (BMSCs), osteoclasts (Roodman, 2008), myeloid cells, and immune effector cells. BMSCs promote growth and drug resistance in MM cells; however, the functional significance of other BM cellular components is unclear.

Macrophages and dendritic cells (DCs) regulate tumor cell growth (Banchereau and Steinman, 1998; Kukreja et al., 2006; McKenna et al., 2005; Ribatti et al., 2006). DCs are BM-derived mononuclear cells (MNCs) that also play an essential role in immune responses (Steinman and Cohn, 1973). In humans, two major DC subsets have been identified based on their origin, phenotype, and function (Colonna et al., 2004; O'Doherty et al., 1994): myeloid DCs (mDCs) ($CD11c^+$, $CD123^-$) that include Langerhans cells and interstitial DCs, and plasmacytoid dendritic cells (pDCs) (Grouard et al., 1997). pDCs lack lineage

SIGNIFICANCE

Recent reports demonstrate infiltration of dendritic cells (DCs) at tumor sites, but with unclear significance. Here we show the pathophysiologic role of plasmacytoid DCs (pDCs) in multiple myeloma (MM). Our study shows increased numbers and more frequent localization of pDCs in MM patient BM than normal BM. Functional analysis using in vitro and in vivo models of human MM in the BM milieu shows that pDCs confer growth, survival, chemotaxis, and drug resistance. Importantly, targeting Toll-like receptors with CpG ODNs improves immune function of pDCs and abrogates pDC-induced MM cell growth. These findings identify an integral role of pDCs in MM pathogenesis and provide the basis for targeting pDC-MM interactions as therapeutic strategy to improve patient outcome.

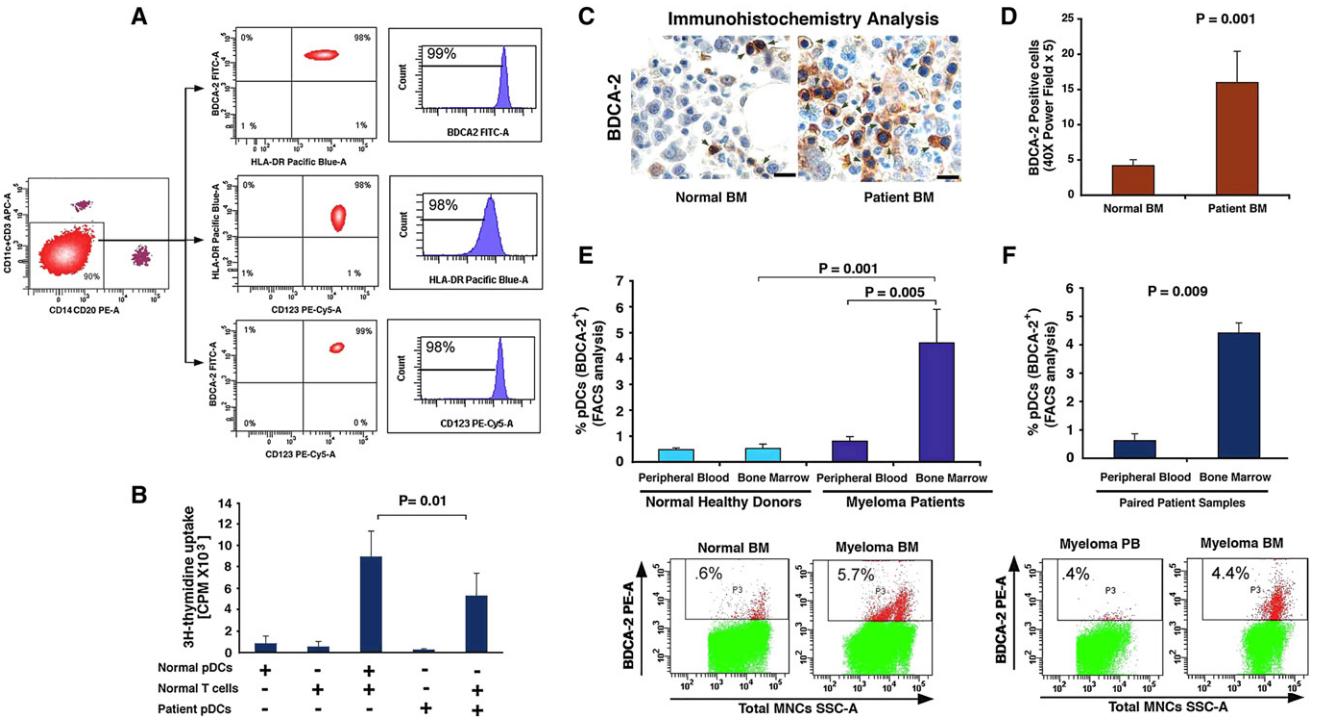

Figure 1. Distribution and Frequency of pDCs

(A) Total MNCs were subjected to BDCA-4-positive selection with two-step purification, and then labeled with CD123 PE-Cy5, HLA-DR Pacific Blue, BDCA-2 FITC, CD14-PE, CD20 PE, CD11c, and CD3 APC antibodies. Lin$^-$, and CD11c$^-$ (90%) cells were gated and FACS sorted. Analysis of this cell population showed 99% BDCA-2$^+$, 98% HLA-DR$^+$, and 98% CD123$^+$ cells.

(B) DNA synthesis in allogeneic T cells stimulated by pDCs from healthy donors and MM patients (mean ± standard deviation [SD]; n = 4).

(C) IHC analysis on normal donor BM and MM patient BM biopsies was performed using BDCA-2 antibody. Arrows indicate brown BDCA-2-positive pDCs. Micrographs are representative from ten MM patients and five normal donors. Scale bars represent 10 μM.

(D) Quantification of BDCA-2-positive pDCs in MM BM versus normal BM from (C). The pDC frequency was quantified by selecting five random independent high-power (×40) microscopic fields for each tissue sample.

(E) Quantification of pDCs from normal donors PB and BM versus MM patient PB and BM by FACS using BDCA-2-PE conjugated antibody. In the upper panel, data shown were derived from analysis of 32 MM patients and 8 normal donors. In the lower panel is a representative FACS analysis showing a higher percentage of BDCA-2-positive pDCs in MM BM versus normal BM.

(F) The upper panel shows quantification of pDCs from matched paired samples of eight MM patient PB and BM by FACS using BDCA-2 antibody. In the lower panel, a representative FACS analysis from eight patients analyzed is shown. Error bars indicate SD.

cell markers for T, B, NK cells, and monocytes, and express CD123, HLA-DR, and BDCA-2 (Colonna et al., 2004; Dzionek et al., 2002; Grouard et al., 1997; O'Doherty et al., 1994). Stimulated pDCs have strong antigen-presenting potential, and regulate antiviral innate immunity (Gilliet et al., 2008; Krieg, 2007; Siegal et al., 1999). Prior studies showed that pDCs from MM patients are defective in their antigen-presenting function (Brimnes et al., 2006; Ratta et al., 2002). Indeed, loss of immune function of tumor-infiltrating DCs has been linked to the suppressive effects of the tumor microenvironment mediated via vascular endothelial growth factor (VEGF), interleukin-6 (IL-6), or macrophage stimulating factor (MCSF) in cancers (Zou, 2005), including MM (Hayashi et al., 2003). Importantly, pDCs play a role in normal B cell development into plasmablasts, their differentiation into antibody-secreting plasma cells, and their survival (Garcia De Vinuesa et al., 1999; Jego et al., 2003; Poeck et al., 2004; Tabera et al., 2008). However, the role of pDCs in regulating growth and survival of malignant plasma cells is unclear. In the present study, we have characterized the distribution/frequency and function of pDCs in MM.

RESULTS AND DISCUSSION

Distribution and Frequency of pDCs in MM

MM is characterized by immune dysfunction (Brown et al., 2001; Ratta et al., 2002). We first examined the immune function of pDCs derived from normal donors versus MM patients (defined in Figure 1A as HLA-DR$^+$ CD123$^+$ BDCA-2$^+$ cells) by their ability to stimulate allogeneic T cell response. Even though resting pDCs are known poor antigen-presenting cells (Liu, 2005), a comparative analysis of MM BM pDCs versus normal pDCs shows markedly decreased ability of MM BM pDCs to trigger T cell proliferation versus normal pDCs (p = 0.01).

Recent reports linked increased infiltration of pDCs in human tumors (Liu, 2005), but with unclear significance. Studies related to the distribution of pDCs in MM are limited and unclear. For example, one study observed a decreased number of pDCs in peripheral blood (PB) from MM patients compared with PB from normal donors (Brimnes et al., 2006), whereas another study showed that PB-derived pDCs from MM patients are numerically within the normal range (Brown et al., 2001). We

therefore next examined the distribution and frequency of pDCs in MM patients versus normal donors using immunohistochemical analysis of biopsy samples and fluorescence-activated cell sorting (FACS) analysis of freshly obtained samples. For these studies, we utilized antibody against pDC specific marker BDCA-2 (Dzionek et al., 2001). We examined ten MM patient and five normal donor BM biopsy specimens for the expression of BDCA-2 by immunohistochemistry analysis. Figure 1C is a representative photograph showing pDCs as BDCA-2-positive stained (brown) cells. These cells were then quantified in all MM patient and normal samples (Figure 1D); pDCs were increased in MM BM versus normal BM. We then utilized FACS analysis to determine the frequency of pDCs in freshly obtained samples using BDCA-2 antibody. We examined BM samples from 32 MM patients with newly diagnosed and relapsed/refractory disease, as well as samples from eight normal donors. Comparative analysis shows 4.7% ± 0.8% pDCs in MM BM versus 0.4% ± 0.2% in normal donor BM (Figure 1E). In contrast, no significant difference in pDC number was observed between normal BM versus PB (Figure 1E, eight normal donors). Furthermore, increased pDCs were noted in MM BM versus MM PB. Analysis of pDCs in matched BM and PB samples from eight patients confirmed increased numbers of pDCs in BM than in PB (4.4 ± 0.3% in BM versus 0.62 ± 0.24% in PB, Figure 1F). These findings suggest that (1) increased numbers of pDCs are present in MM patient BM versus normal BM; and (2) pDCs are more frequently localized in MM BM than MM PB.

pDCs Trigger Growth and Prolong Survival of MM Cells

We next examined the functional significance of increased pDC numbers in MM BM. Our prior studies showed that BMSCs trigger MM cell growth; therefore, we examined whether pDCs similarly affect MM cells. MM.1S cells and normal PB pDCs were cultured either alone or together at 1:3, 1:5, or 1:7 (pDC:MM) ratio for 24 hr, 72 hr, and 120 hr, and DNA synthesis was measured by ^{3}H-thymidine (^{3}H-Tdr) uptake. A significant increase in DNA synthesis was noted when MM cells were cultured with pDCs at 1:5 (pDC/MM) ratio: for example, a 3- to 4-fold increased ^{3}H-Tdr uptake was found in MM.1S cells cultured with pDCs for 72 hr versus control MM cells alone ($p < 0.005$) (Figure 2A). No increase in DNA synthesis was observed in pDCs cultured alone (Figure 2A). Coculture of pDCs with MM.1S cells at 1:3 or 1:7 (pDC/MM) ratio also induced MM.1S cell growth (data not shown); however, maximal growth was noted at 1:5 pDC/MM ratios. This 1:5 pDC/MM ratio is physiologically relevant because pDC frequency in MM BM is 4.7% ± 0.8% (Figure 1E) corresponding to 23.5% ± 3% MM cells in BM. Coculture of green fluorescent protein (GFP)-expressing MM.1S cells with pDCs increased number of GFP^{+} cells, suggesting that pDCs induce MM.1S cell growth (Figure 2B). Irradiated pDCs retain their ability to trigger MM cell proliferation (Figure 2C). To determine whether pDCs alter the clonogenic growth of MM cells, we plated MM.1S cells with pDCs in methylcellulose cultures. pDCs markedly increase the number of tumor colonies versus tumor cells alone (Figure 2D). This MM cell growth promoting activity of pDCs was further confirmed by additional assays. For example, WST proliferation assay also showed that pDCs trigger proliferation of MM cells (Figure 2E). Finally, pDC-induced MM cell growth was associated with activation of growth signaling kinase ERK in MM.1S cells (Figure 2F). Together, these findings demonstrate that pDCs can promote MM cell growth.

Our prior studies showed that BMSCs trigger MM cell growth (Hideshima et al., 2007). A recent study showed that in vitro-generated mDCs enhance clonogenicity of MM cells (Kukreja et al., 2006). We therefore examined the stimulatory effect of normal PB mDCs versus pDCs versus MM patient BMSCs on MM cell growth. Culture of MM.1S cells with BMSCs triggered a 2.2 ± 0.7-fold increase in DNA synthesis in MM.1S cells. Importantly, pDCs triggered 3.1 ± 0.3-fold increased DNA synthesis, whereas mDCs induced only 15%–20% increased DNA synthesis (Figure 2G). These data suggest that BMSCs and mDCs also stimulate DNA synthesis, albeit to a lesser extent than pDCs. The differences in the potency of pDC versus mDCs in our study versus a previous report (Kukreja et al., 2007) may be due to the use of different MM cell line, sources of pDCs, and/or growth assays. Nonetheless, both studies suggest a role of DCs in modulating MM cell growth. Additionally, pDCs are more robust growth stimulators of MM cells than monocytes under similar experimental conditions (see Figure S1 available online). Importantly, the pDC-depleted BM cells did not trigger significant DNA synthesis in MM cells (Figure 2H). Similarly, coculture of pDC-depleted BM cells with GFP-MM.1S cell showed no increase in GFP^{+} cell numbers (data not shown), confirming the specific MM cell growth-promoting activity of pDCs.

Genetic heterogeneity (Bergsagel and Kuehl, 2005) and drug resistance in MM impact the interaction of tumor cells with BMSCs and its functional sequelae (Hideshima et al., 2007). We examined the growth-promoting activity of pDCs in a broader panel of MM cell lines, including those that are drug resistant and cytogenetically distinct. These included Dex-resistant MM.1R cell line with t14;16 translocation; parental RPMI-8266 cell line and its doxorubicin-resistant derivative (8226/Dox-6); an IL-6-dependent cell line INA-6; and OPM-2 (t4:14) MM cell line. pDCs stimulated DNA synthesis in all MM cell lines, albeit to a differential extent (Figure 2I). These findings suggest that genetic heterogeneity in MM may be associated with differential tumor growth responses to pDCs.

Patient MM cells have a low proliferative capacity in vitro, and we similarly examined the effects of pDCs on primary tumor cells. Our results show that pDCs trigger proliferation of patient MM cells (Figure 3A), evidenced by increase in DNA synthesis. In contrast, pDCs had little, if any, effect on DNA synthesis in normal plasma cells (Figure 3A). Similar results were obtained with viability assays (data not shown).

We next examined whether MM patient pDCs, like normal donor pDCs, trigger proliferation of MM cell line and patient MM cells. MM patient-derived BM pDCs induced growth of both allogeneic MM.1S cell line (Figure 3B), and autologous tumor cells (Figure 3C). Importantly, we found a significant increase in the survival of patient MM cells when cocultured with pDCs for 3–4 weeks (Figure 3D; 35%–50% increase in five of five patients cells, $p < 0.05$). Immunostaining with kappa and lambda immunoglobulin G (IgG) antibodies confirmed the clonality of MM cells in prolonged cultures with pDCs (Figure 3E).

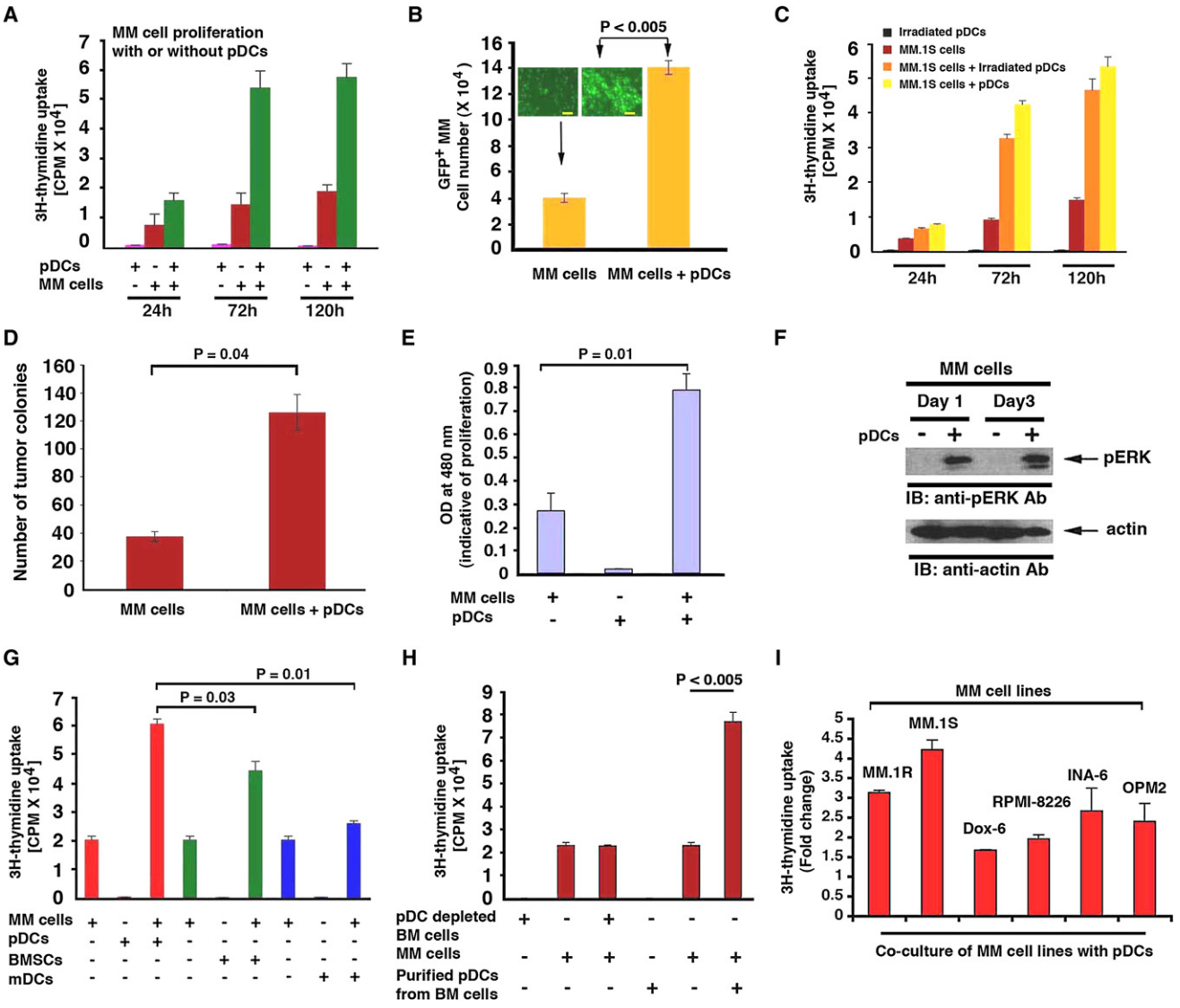

Figure 2. pDCs Induce MM Cell Growth

(A) MM.1S cells (5 × 10^4 cells/200 μl) and pDCs (1 × 10^4 cells/200 μl) were cultured either alone or together for indicated intervals, and then analyzed for DNA synthesis using ^{3}H-TdR uptake (mean ± SD; n = 3).

(B) GFP$^+$ MM.1S cells were cultured either alone or with pDCs for 3 days; GFP$^+$ MM.1S cells were counted under fluorescent microscope (mean ± SD; n = 2). The inset shows a micrograph from the experiment (scale bars represent 40 μM).

(C) MM.1S cells were cultured alone or together with either irradiated or nonirradiated pDCs for indicated intervals, and analyzed for growth (mean ± SD; n = 2).

(D) MM.1S cells were plated with or without pDCs. The numbers of tumor colonies were enumerated using microscopy after incubation for 10–14 days (mean ± SD; n = 2).

(E) MM.1S cells and pDCs were cultured as in (A) for 72 hr and analyzed for growth by WST assays (mean ± SD; n = 3).

(F) MM.1S cells (2.5 × 10^6) and pDCs (0.5 × 10^6) were cultured as in (A); MM.1S cells were separated from pDC cocultures with CD138 microbeads and analyzed for ERK activation by immunoblotting.

(G) MM.1S cells, pDCs, mDCs, or MM patient-BMSCs were cultured either alone or together at 1:5 (pDC/MM, mDC/MM or BMSC/MM) ratio for 3 days, and DNA synthesis was measured using ^{3}H-TdR uptake (mean ± SD; n = 3).

(H) pDC-depleted MM BM cells versus purified MM BM pDCs were examined for their stimulatory effect on MM.1S cell growth (mean ± SD; n = 2).

(I) MM cell lines were cultured either alone or together with pDCs for 3 days, and analyzed for DNA synthesis by ^{3}H-TdR uptake assay. Data are presented as fold change in DNA synthesis in the presence versus absence of pDCs (mean ± SD; $p < 0.05$; n = 3). Normal PB pDCs were utilized in experiments shown in (A)–(I). Cocultures of pDCs and MM cells were performed using 1:5 (pDC/MM) ratio. Growth assays were performed using 1 × 10^4 pDCs and 5 × 10^4 MM cells in 200 μl media in 96-well plates. Error bars indicate SD.

pDCs Confer Drug Resistance

Binding of MM cells to BMSCs mediates resistance to conventional (dexamethasone) therapies; and conversely, novel therapies (bortezomib, lenalidomide) can overcome this growth advantage conferred by BMSCs (Hideshima et al., 2007). We therefore next determined whether various anti-MM agents

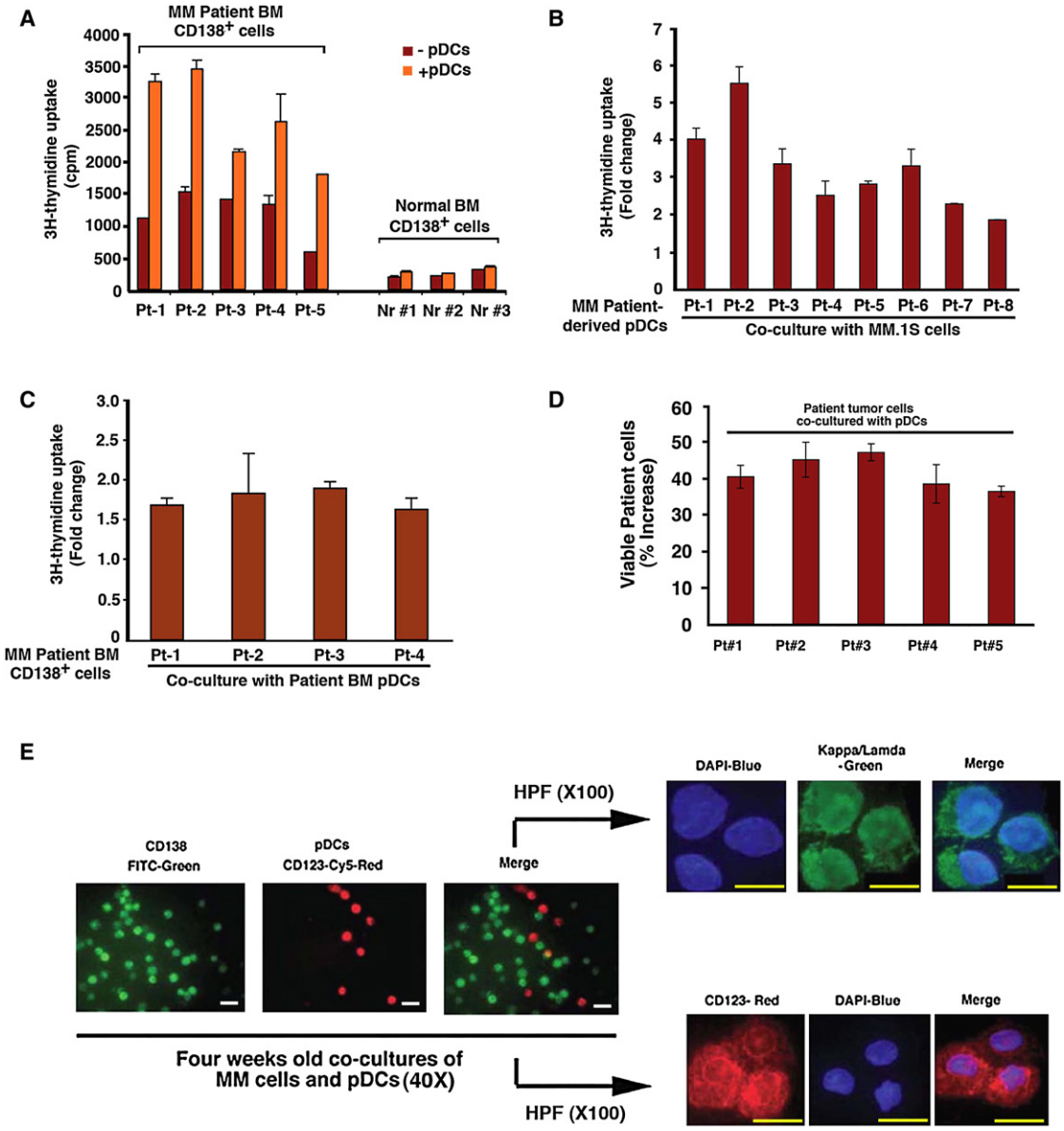

Figure 3. Effect of pDCs on Patient MM Cells

(A) Purified patient MM cells and normal BM plasma cells from healthy donors were cultured with or without pDCs for 3 days, and DNA synthesis was measured by ^{3}H-TdR uptake (mean ± SD of triplicate cultures; $p < 0.05$ for all samples; pDC/MM ratios: patient number (pt#) 1–3 at 1:5, pt#4 at 1:2, and pt#5 at 1:3).

(B) MM.1S cells were cultured as in Figure 2A with or without patient BM pDCs for 3 days, and analyzed for growth by ^{3}H-TdR uptake (mean ± SD of triplicate cultures; $p < 0.005$ for all samples).

(C) Patient MM cells were cultured with or without autologous BM pDCs for 3 days, and DNA synthesis was measured by ^{3}H-TdR uptake (mean ± SD of triplicate cultures; $p < 0.004$ for all samples; pDC/MM ratio: pt#1–4 at 1:5). Data (B and C) are presented as fold change in DNA synthesis in the presence versus absence of patient BM pDCs.

(D) Normal PB pDCs and patient MM cells were cocultured in DCP-MM medium at 1:5 (pDC/MM) ratio for 3 weeks, and viable cells were quantified by trypan blue exclusion assay. Data are presented as percent increase in survival of tumor cells in the presence versus absence of pDCs (mean ± SD of duplicate cultures; $p < 0.05$).

(E) Normal PB pDCs and patient MM cells were cocultured as in (D) for 4 weeks and then stained with CD138-FITC antibody, CD123-PE antibody, kappa/lambda antibody, and DAPI. The micrograph shown is representative of five experiments with similar results. Scale bars represent 20 μM (left three panels) and 10 μM (right, upper, and lower panels). Error bars indicate SD.

overcome pDC-mediated biologic sequelae in MM cells. We asked (1) whether the anti-MM agent bortezomib directly affects the viability of pDCs; and (2) whether pDC-triggered growth of MM cells is affected by bortezomib. Treatment of normal PB pDCs for 24 hr with bortezomib (20 nM) did not significantly decrease their viability (Figure 4A). Similarly, treatment of pDCs with even higher doses of bortezomib (20–100 nM) did not trigger significant apoptosis (Figure 4B). Longer periods (48 hr) and

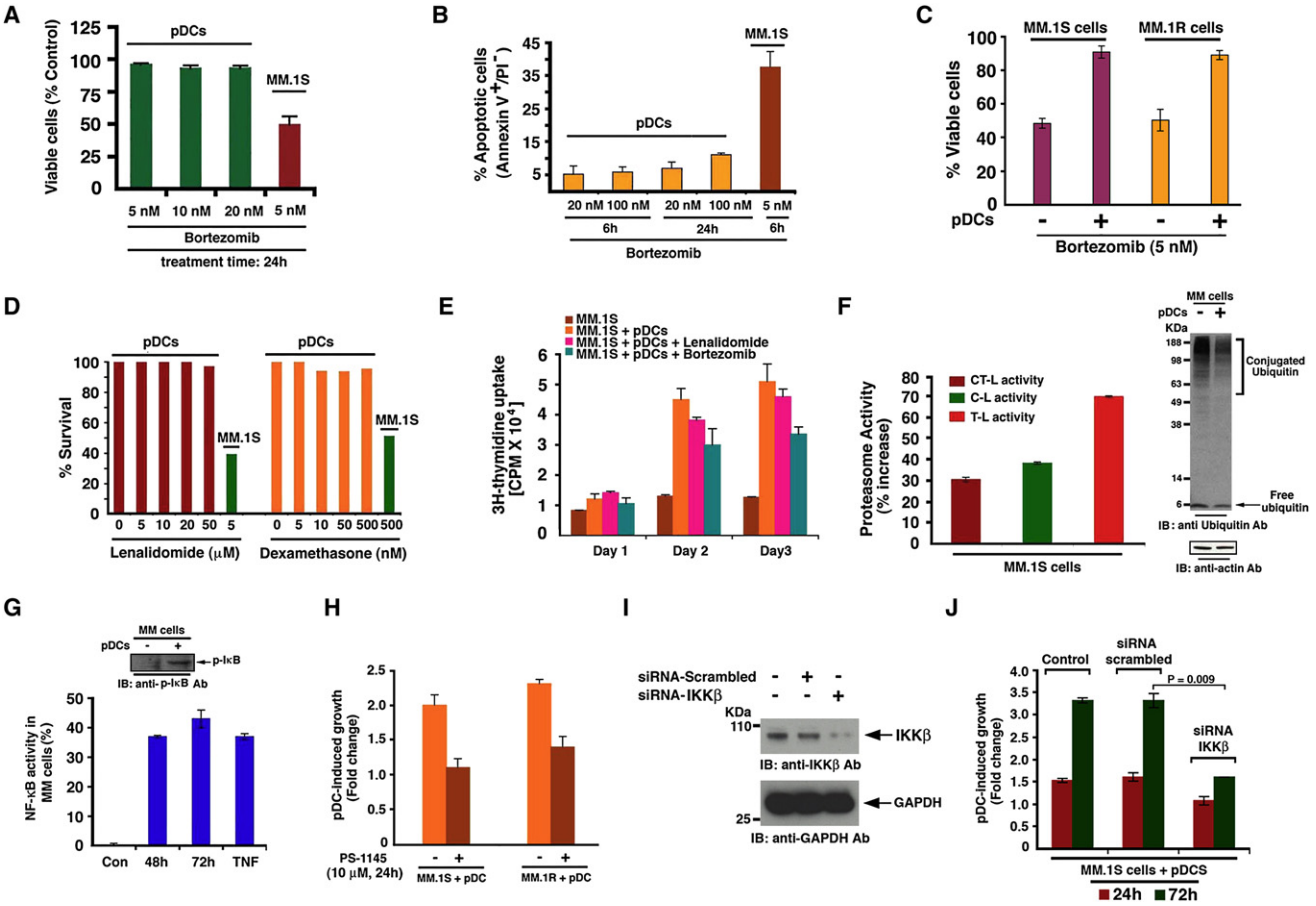

Figure 4. pDCs Confer Drug Resistance in MM Cells

(A and B) pDCs (1×10^6 cells) were treated for the indicated time and concentrations of bortezomib and then analyzed for viability and apoptosis by MTT and Annexin V/PI staining assays (mean ± SD; $p < 0.005$; n = 4).

(C) MM.1S and MM.1R cells were treated with bortezomib in the presence or absence of pDCs for 24 hr, and analyzed for viability (mean ± SD; $p < 0.05$; n = 4).

(D) pDCs were treated with indicated agents for 24 hr, and then analyzed for viability (mean ± SD; $p < 0.05$; n = 3).

(E) MM.1S cells or MM.1S plus pDCs were cultured in the presence or absence of bortezomib (5 nM) or lenalidomide (5 μM), and analyzed for DNA synthesis by ^{3}H-TdR uptake assay (mean ± SD; $p < 0.05$; n = 3).

(F) MM.1S cells were cultured with pDCs for 72 hr, separated with CD138 microbeads, and harvested; protein extracts were analyzed for proteasome activity. Data are presented as percent increase in proteasome activities in the presence versus absence of pDCs (mean ± SD; $p < 0.005$; n = 3). Similarly, pDC-induced alteration in protein ubiquitination in MM.1S cells was assessed by immunoblotting.

(G) MM.1S cells were cultured as in (F) and analyzed for NF-κB activity with p65 ELISA assay (mean ± SD; $p < 0.05$, n = 3). As shown in the inset, MM.1S cells cultured with or without pDCs were analyzed for p-IκB levels by immunoblotting.

(H) MM.1S or MM.1R cells were cultured with pDCs in the presence or absence of PS-1145, and then analyzed for growth (mean ± SD; $p = 0.01$ for MM.1S and $p = 0.02$ for MM.1R cells; n = 2).

(I) MM.1S cells were transfected with siRNA IKKβ (0.8 μM) or scrambled siRNA for 48 hr and harvested; protein extracts were subjected to immunoblot analysis with anti-IKKβ or anti-GAPDH antibodies.

(J) MM.1S cells were transfected with siRNA IKKβ or scrambled siRNA, followed by coculture with pDCs for indicated times; and then analyzed for growth using WST proliferation assay (mean ± SD; n = 2). Normal PB pDCs were utilized in experiments shown in (A)–(J) at 1:5 pDC/MM ratio. Culture medium is described in Experimental Procedures. Error bars indicate SD.

higher dose of bortezomib triggered cell death of pDCs (data not shown), as also reported in a prior study (Kukreja et al., 2007). However, it is noteworthy that MM cells require many fold lesser concentrations of bortezomib and shorter periods of exposure to undergo apoptosis (e.g., IC_{50} for MM.1S cells is 5 nM at 24 hr, as in Figures 4A and 4B), suggesting that pDCs are relatively resistant to bortezomib compared to tumor cells. Importantly, and in agreement with a previous report (Kukreja et al., 2007), we found that pDCs protect MM cells against bortezomib-induced cytotoxicity (Figure 4C). Furthermore, pDCs triggered MM cell proliferation even in the presence of bortezomib, albeit to a lesser extent than without drug (Figure 4E). As with bortezomib, treatment of pDCs with immunomodulatory drug lenalidomide does not significantly decrease their viability (Figure 4D). Moreover, pDCs triggered increased DNA synthesis in MM cells even in the presence of lenalidomide (Figure 4E). Conventional agent Dex (0.5 μM) triggered only 8%–10% decreased viability of pDCs (Figure 4D), with 12%–15% apoptosis. Importantly, similar

concentrations of Dex triggered 70% ± 3.6% apoptosis in MM cells (data not shown). We therefore conclude that in comparison to tumor cells, pDCs are relatively resistant to bortezomib, lenalidomide, and Dex therapies.

We next performed microarray analysis to identify the molecular mechanisms whereby pDCs confer growth and drug resistance in MM cells. For these studies, we examined pDC-induced gene changes in MM cells. In particular, we found that pDCs triggered upregulation of transcripts mediating proteasome function in MM.1S cells, including proteasome 26S subunit and PA200 (ATPase complex) (Figure S2). Furthermore, a marked increase in chymotrypsin-like (CT-L), caspase-like (C-L), and trypsin-like (T-L) proteasome activity, was noted in MM.1S cells cultured with pDCs versus MM.1S cells alone (Figure 4F). In concert with these findings, pDCs triggered a decrease in protein ubiquitination in MM.1S cells (Figure 4F). Bortezomib primarily blocks CT-L and C-L, but not T-L activity, and pDCs significantly increase T-L activity in MM cells. Importantly, bortezomib-induced cytotoxicity is linked to inhibition of proteasome activity (Chauhan et al., 2005), and our data suggest that pDCs upregulate proteasome activity. It is therefore likely that pDCs, by enhancing proteasome activity in MM cells, raise the IC_{50} of bortezomib for MM cells. A recent study also showed that overexpression of proteasome subunit confers resistance to bortezomib (Oerlemans et al., 2008). These data suggest a likely mechanism whereby pDCs confer bortezomib resistance in MM cells.

Besides the proteasome components, pDCs also increased transcripts linked to nuclear factor (NF)-κB signaling pathway in MM cells including, NF-κB activating protein and genes containing NF-κB consensus binding sites in their promoter regions (e.g., IL-6, VEGF, IL-10). NF-κB mediates growth, survival, and drug resistance in MM cells (Chauhan et al., 1996). DNA binding enzyme-linked immunosorbent assay (ELISA) and immunoblotting confirmed pDC-induced NF-κB activation in MM.1S cells (Figure 4G and inset). Importantly, blockade of NF-κB using IKK inhibitor PS-1145 decreases pDC-triggered MM.1S and MM.1R cell growth (Figure 4H). To further confirm the role of NF-κB in mediating pDC-induced MM cell growth, we knocked down IKKβ expression in MM cells using siRNA. The functional specificity of IKKβ siRNA was evident by a marked decrease in-protein levels of IKKβ (Figure 4I). Transfection of IKKβ siRNA, but not negative-control (scrambled) siRNA, significantly inhibited pDC-induced growth in MM.1S cells (Figure 4J). Together, these findings suggest an obligatory role of NF-κB during pDC-triggered MM cell growth.

Chemotaxis/Migration during pDC-MM Interaction

The frequent localization of pDCs in MM BM and their ability to trigger MM cell growth suggest involvement of chemotaxis between pDCs and MM cells. Time-lapse live cell imaging demonstrates increased motility of pDCs and MM cells toward each other, evidenced by formation of filopodia (Figure 5A and Movie S1). In agreement with these data, Transwell insert assays demonstrate markedly increased migration of MM.1S cells toward pDCs (Figure 5B, left panel). Importantly, 2- to 3-fold greater numbers of MM.1S cells migrated toward supernatants from pDC-MM cultures compared to those from cultures of pDCs or MM.1S cells alone (Figure 5B, right panel). Crystal violet staining confirms increased numbers of MM.1S cells migrating toward supernatants from pDC-MM cultures (Figure 5B, micrographs). Similarly, pDCs showed increased migration toward supernatants of pDC-MM cocultures (data not shown). These findings demonstrate chemotaxis between pDCs and MM cells and, importantly, show that pDC-MM interaction further enhances secretion of chemotactic factors.

Role of Soluble Factors

We next directly analyzed secretion of cytokines and chemokines in supernatants from pDCs, MM.1S cells, and pDC-MM.1S cell cocultures using cytokine bead arrays. pDC-MM interaction triggers secretion of many known MM cell growth and chemotactic factors (Hideshima et al., 2007) including IL-10, VEGF, CD40L, IL-8, IL-15, IL-6, and MCP-1 or IP10 (Figures 5C–5E). We also found that pDC-MM interaction increased IL-3 and SDF-1α (CXCL12) levels (Figure 5F). Both IL-3 and SDF-1α mediate autocrine growth and chemotaxis in MM cells (Hideshima et al., 2007; Lee et al., 2004). SDF-1α is involved in in vivo migration of pDCs into tumors via its ligand CXCR4 (Zou et al., 2001). Importantly, blockade of IL-3 or SDF-1α with neutralizing antibodies or AMD3100 (drug targeting CXCR4-CXCL12) markedly abrogates pDC-induced MM cell growth (Figure 5G). IL-3 is a survival factor for pDCs (Grouard et al., 1997). Our finding that MM cells secrete low levels of IL-3 constitutively, which is markedly increased upon interaction with pDCs explains, at least in part, prolonged survival of pDCs when cultured with MM cells in vitro (Figure 3E).

We next assessed whether pDCs migrate in response to chemokines identified in cytokine bead arrays. Transwell insert assays show significant chemotaxis of pDCs toward CXCL12 (SDF-1α), IL-3, CXCL10 (IP-10), CCL4 (MIP1α), CCL3 (MIP1β), and MCP-1 (Figure 5I). These data suggest that pDC-MM interaction upregulates many chemokines that may allow for pDCs migration and homing of pDCs to MM BM.

Requirement of pDC-MM Cell Contact

To determine whether cell-cell contact between pDCs and MM cells is required, we utilized Transwell Inserts assays, immunofluorescence (IFC) with confocal microscopy, and immunohistochemistry (IHC) analysis. Culture of pDCs and MM cells in the transwell system, which prevents physical interaction of pDCs with MM cells while allowing for proximity and stimulation by soluble factors, significantly attenuated the ability of pDCs to trigger MM cell proliferation (Figure 6A). These findings suggest that contact-dependent secretion of soluble factors accounts for the majority of pDC-induced MM cell growth.

To determine whether pDCs are indeed in close proximity to MM cells in vivo, we examined BM biopsy samples from MM patients. Patient BM biopsies were subjected to dual IFC staining with BDCA-2 (pDCs) and CD138 (MM cells) and DAPI. Results demonstrates direct cell-cell contact between pDCs and MM cells as well as clusters of pDCs with MM cells (Figure 6B). IHC analysis with another pDC marker CD123 confirmed these data (Figure S3).

Adhesion of MM cells to BMSCs triggers transcription and secretion of soluble factors that mediate MM cell growth in

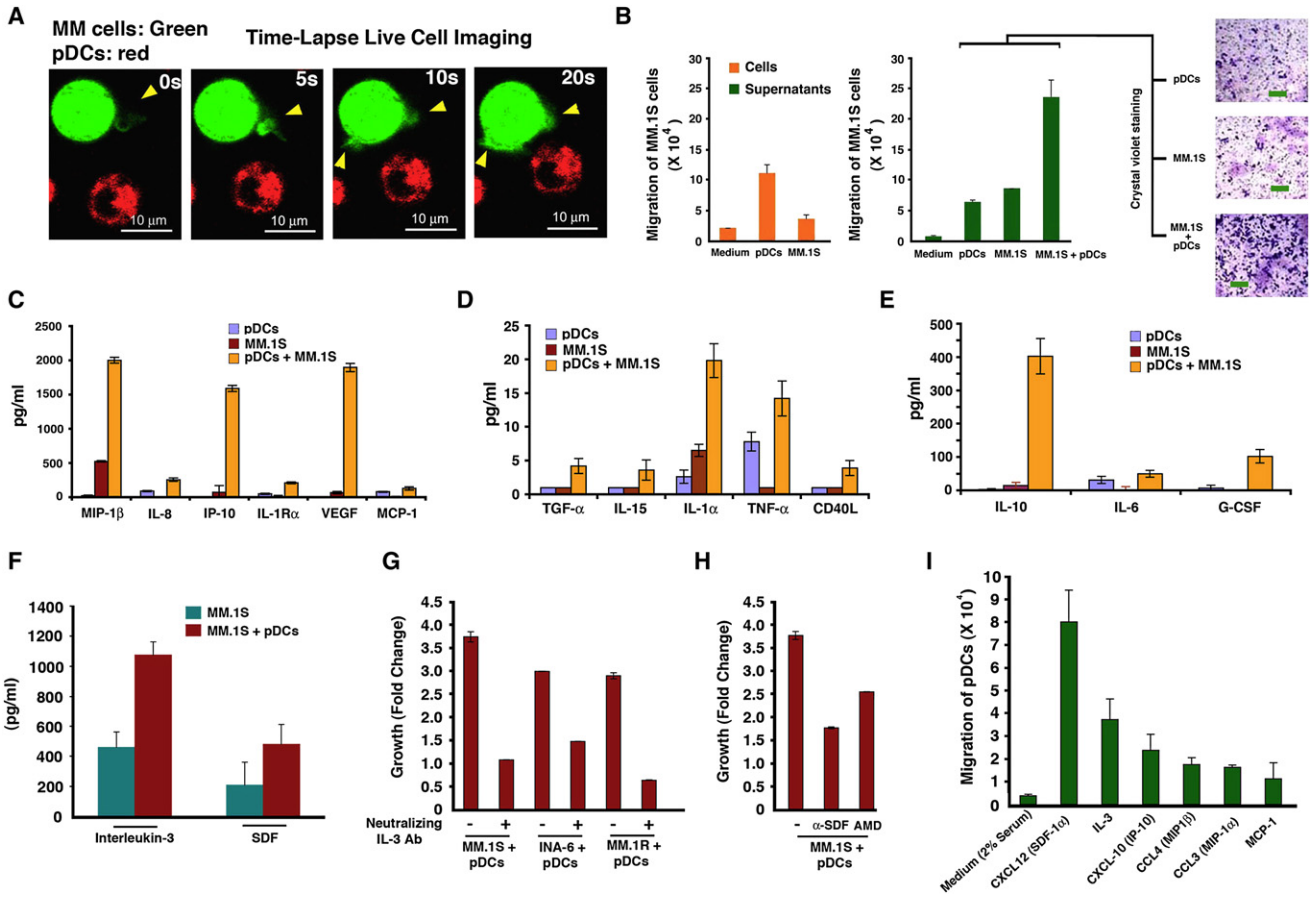

Figure 5. Chemotaxis/Migration of MM Cells and Role of Soluble Factors in pDC-MM Interactions

(A) Representative examples of frames from time-lapse imaging of pDC-MM coculture are shown to demonstrate chemotactic activity between pDCs and MM cells, as evidenced by formation of filopodia (yellow arrowheads). Images were taken for 30 ms interval for 5–15 min. The video is available in Supplemental Data (Movie S1).

(B) Migration assays: MM.1S cells were seeded in the upper compartment; the lower chamber contained medium alone, pDCs, MM.1S cells, supernatants from pDCs, supernatants from MM.1S cells, or supernatants from 3 day cocultures of pDCs and MM.1S cells. The migrated cells were quantified and presented as bar graph (mean ± SD; $p < 0.005$; n = 2). Micrographs shows crystal violet staining of migrated cells. Scale bars represent 40 μM.

(C–E) MM.1S cells were cultured with pDCs for 72 hr as described in Experimental Procedures; supernatants were collected and subjected to cytokine bead arrays (mean ± SD; n = 4).

(F) MM.1S cells were cultured with or without pDCs for 72 hr; supernatants were analyzed for IL-3 and SDF-1α levels using ELISA (mean ± SD; $p = 0.05$ for both IL-3 and SDF-1α; n = 5).

(G) MM.1S, INA-6 (with rhIL6 2.5 ng/ml), and MM.1R cell lines were cultured with pDCs in the presence or absence of anti-IL-3 antibody (10 ng/ml) for 72 hr, and analyzed for growth by WST proliferation assays (mean ± SD; $p < 0.005$; n = 3).

(H) MM.1S cells were cultured with pDCs in the presence or absence of anti-SDF-1α (100 ng/ml) or AMD3100 (10 μM), and analyzed for growth by WST proliferation assay (mean ± SD; $p < 0.005$; n = 3).

(I) Transwell insert assays showing migration of pDCs toward chemokines (described in Experimental Procedures). The indicated chemokines were added to the lower chamber of transwells, and pDcs were allowed to migrate through 5 μM pore-size filters for 2 hr. Migrated cells were quantified in the fluid phase of the lower chamber (mean ± SD; n = 3). Normal PB pDCs were utilized in experiments shown in (A)–(I) and cultures were at 1:5 (pDC/MM) ratio. Error bars indicate SD.

a paracrine manner (Anderson, 2007). Similarly, we here found that pDC-MM interaction upregulates many MM cell growth, survival, and chemotactic factors. Importantly, although, MM cells constitutively secrete factors, the direct cell-cell interaction between pDCs and MM cells further augments the production of cytokines and chemokines that not only confer growth, survival, and drug resistance in MM cells, but also prolong survival of pDCs. Together, these studies suggest a role of both soluble factors and direct pDC-MM cell-cell contact in mediating MM cell growth and pDC survival.

Role of pDC-MM Cell Surface Receptor-Ligand Interactions

The above findings implicate cell surface molecules in mediating interactions that trigger MM cell growth/survival. Both pDCs and MM cells express molecules that play a role in B cell differentiation and serve as costimulatory molecules; e.g., BAFF/APRIL and RANK-RANKL (MacLennan and Vinuesa, 2002; Roodman and Dougall, 2008). Indeed, we found significantly increased BAFF levels in MM patient versus normal donor serum (Figure 6C), as in our previous report (Neri et al., 2007).

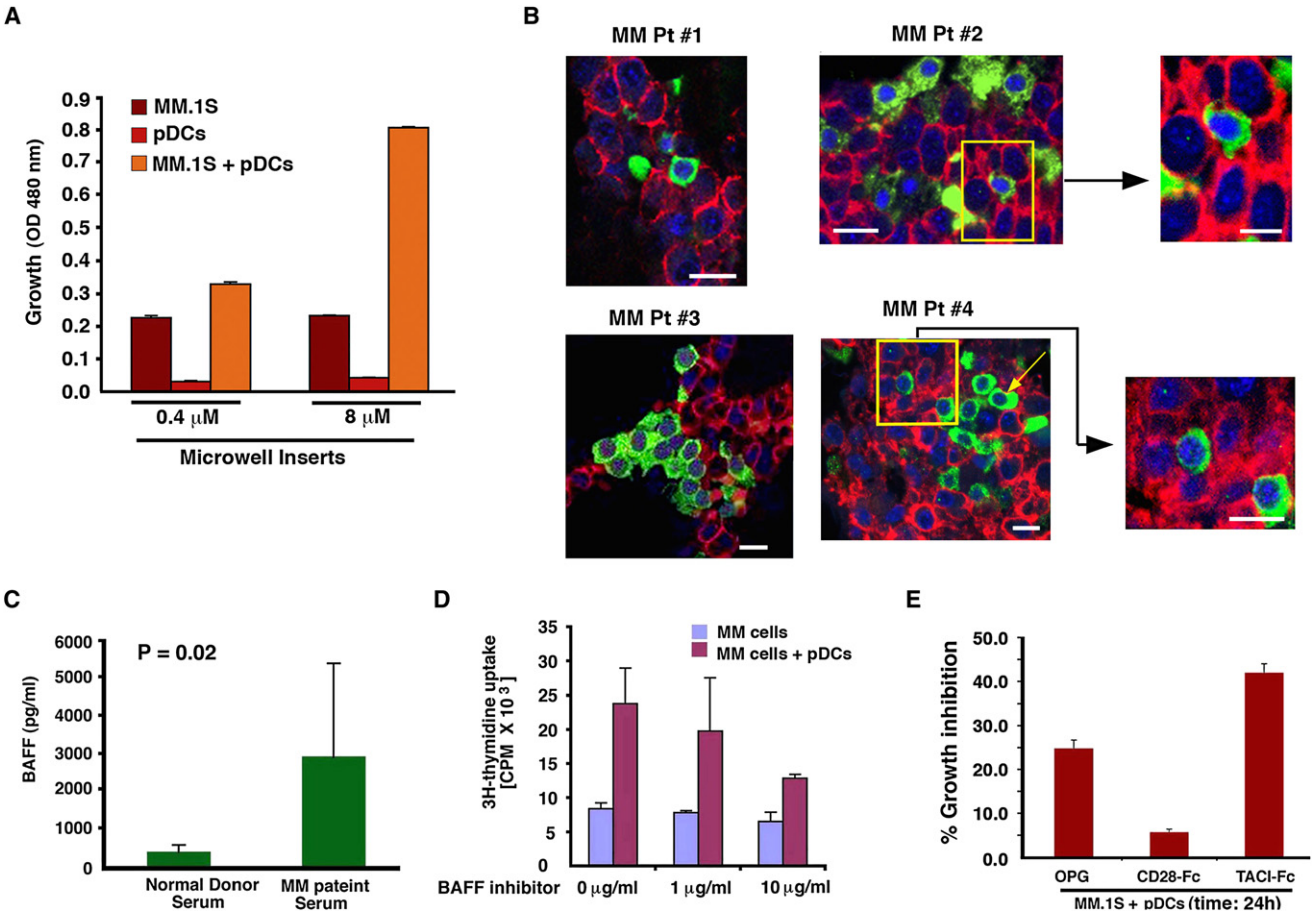

Figure 6. Requirement of pDC Contact with MM Cells

(A) Transwell insert assay: Two different pore size membranes were utilized to separate cells: 0.4 μM (does not allow free passage of cells) and 8 μM (allows cell passage). Normal PB pDC (2×10^4) and MM.1S cells (1×10^5) were added into the upper and lower chamber, respectively, and incubated for 72 hr at 37°C; cells from the lower chamber were then harvested and analyzed for growth by WST assays (mean ± SD; $p = 0.001$; $n = 3$).

(B) Analysis of MM patient BM biopsies (MM #1–MM #4) to show in vivo cell-cell contact between MM BM pDCs with tumor cells. MM patient BM biopsy specimens were subjected to IFC staining for MM cells (CD138 antibody, red) and pDCs (BDCA-2 antibody, green). Nuclear staining was performed with DAPI (blue). Slides were mounted using Vectashield with DAPI. Data shown are representative of 10 MM BM samples analyzed with similar results. Scale bars represent10 μM (MM pt#1–4). The yellow square represents the 3× zoom areas (scale bars represent 5 μM in the upper panel and 10 μM in the lower panel).

(C) BAFF levels were analyzed in serum obtained from five normal and five MM patients with ELISA.

(D) MM.1S cells were cultured either alone or together with normal PB pDCs at 1:5 (pDC/MM) ratio in the presence or absence of BAFF inhibitor at the indicated concentrations for 72 hr and then analyzed for growth (mean ± SD; $p < 0.005$; $n = 3$).

(E) MM.1S cells were cultured with normal PB pDCs at 1:5 pDC/MM ratio in the presence or absence of rhOPG (0.5 μg/ml), TACI-Fc (1 μg/ml), or CD28-Fc (1 μg/ml) for 24 hr, and then analyzed for proliferation (mean ± SD; $p < 0.005$; $n = 2$). Data are presented as percent growth inhibition in pDC-induced MM.1S cell growth in the presence of agents. Error bars indicate SD.

Importantly, blockade of BAFF with either a small-molecule inhibitor or TACI-Fc significantly abrogated pDC-induced MM cell growth (Figures 6D and 6E, respectively). TACI-Fc alone did not affect the viability of MM.1S cells alone (data not shown). In contrast, inhibition of RANK-RANKL with osteoprotegerin also decreased pDC-induced MM cell growth, albeit to a lesser extent than inhibiting BAFF (Figure 6E). Our finding that NF-κB mediates pDC-MM functional sequelae, together with the known role of both BAFF and RANKL in activating NF-κB, suggests the therapeutic potential of targeting BAFF/RANKL in MM. However, it is very likely that other cell surface receptor-ligand interactions are also involved in mediating pDC-MM interactions.

In Vivo Validation of pDC-Induced Growth of MM Cells with MM Xenograft Models

Having defined the functional role of pDCs in regulation of MM biology in vitro, we next examined whether pDCs similarly affect MM cell growth in vivo using murine xenograft models of human MM. In order to evaluate the growth-promoting function of human pDCs within the human BM milieu, we utilized the severe combined immunodeficiency (SCID)-hu model (Tassone et al., 2005), which recapitulates the human BM milieu in vivo. In this model, MM cells are injected directly into human bone chips implanted subcutaneously in SCID mice, and MM cell growth is assessed by serial measurements of circulating levels of soluble

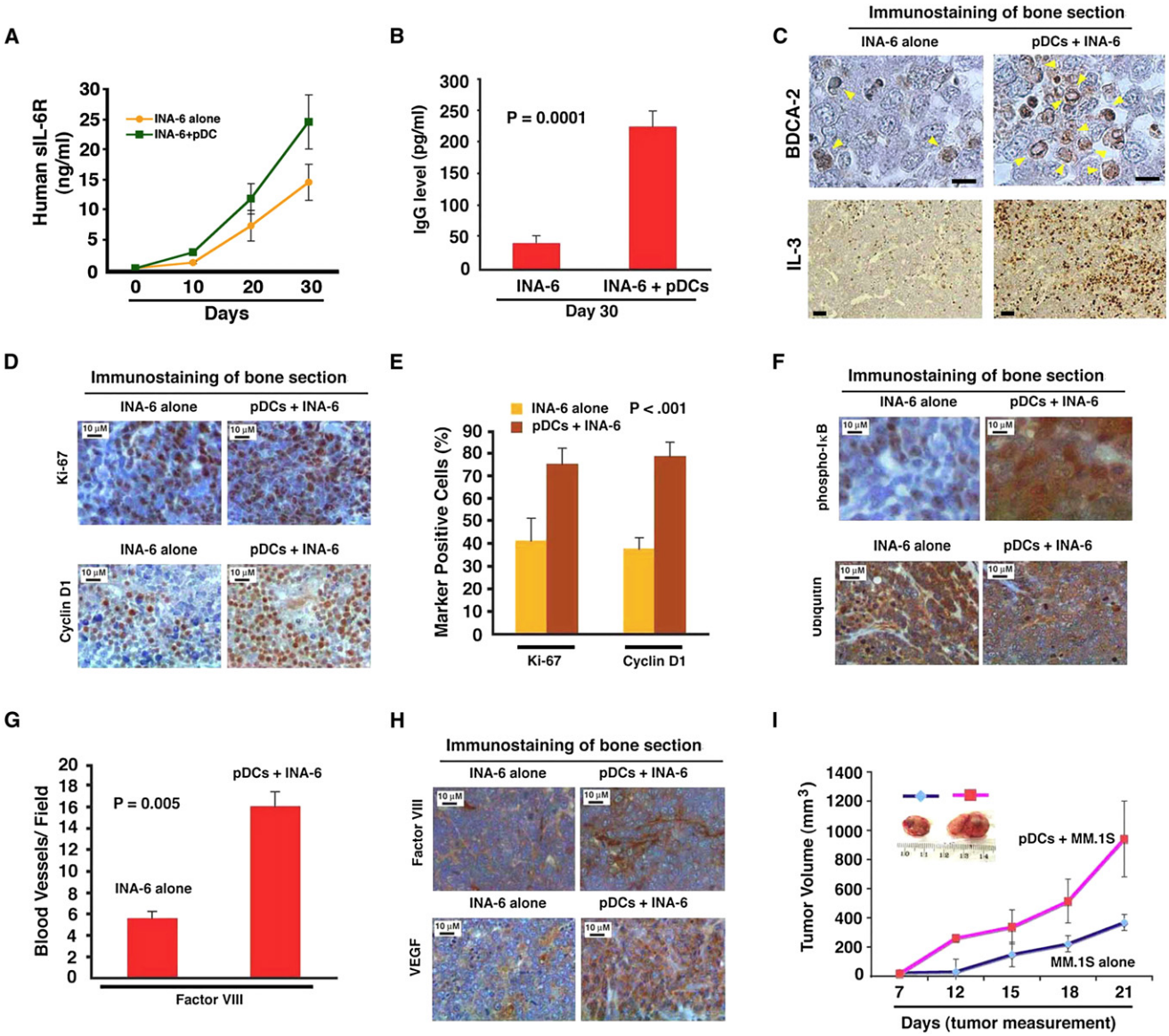

Figure 7. pDCs Enhance Growth of Xenografted Human MM Cells in Mice

(A and B) INA-6 MM cells alone (2×10^6 cells without IL-6), or together with pDCs (0.4×10^6 cells) at 1:5 (pDC/MM) ratio were injected directly into the human fetal bone implant in SCID-hu mice, and mouse sera samples were analyzed for human sIL-6R and Ig by ELISA (mean ± SD; $p < 0.05$; $n = 2$).

(C) Human bone chips were removed from mice 30 days after injection with pDCs and INA-6 cells and immunostained with anti-BDCA-2 and anti-IL-3 antibodies. The scale bar represents 5 μM.

(D–H) Bone sections were immunostained with antibodies against Ki-67, cyclin D1, phospho-IκB, ubiquitin, and factor VIII, and VEGFR1. Dark brown: Marker-positive cells in all cases. Micrographs are representative of bone sections from two different mice in each group.

(E and G) Quantification of Ki-67, cyclin-D1, and factor VIII-positive cells from experiments in (D) and (H) (upper panel).

(I) MM.1S cells alone (2.5×10^6) or together with pDCs (0.5×10^6) (1:5 pDC/MM ratio) were implanted subcutaneously in mice; tumor volume was monitored every third day ($p < 0.05$). Shown in the inset are tumors from mice with either MM.1S or MM.1S cells + pDC. Error bars indicate SD.

human IL-6R and immunoglobulin in mouse serum. A more robust growth of tumor occurred in mice receiving human pDCs and INA-6 MM cells than in mice injected with INA-6 cells alone (Figures 7A and 7B). pDCs alone did not induce tumors in mice (data not shown). Immunostaining of implanted human bone with BDCA-2 showed presence of viable pDCs 30 days after the initial injections (Figure 7C). As in our in vitro results, IL-3 was highly expressed in mice injected with pDCs plus INA-6 cells (Figure 7C). The observation that IL-3 is a survival factor for pDCs, coupled with our in vitro and in vivo results, suggests that IL-3, at least in part, facilitates prolonged survival of pDCs in vivo in the human MM BM milieu.

We also observed an increase in Ki-67 and cyclin D1-positive cells in human bone sections from mice engrafted with pDCs and INA-6 MM cells compared to mice receiving INA-6 cells alone (Figures 7D and 7E). Counterstaining of bone sections with

CD138 confirmed that Ki-67 and cyclin-D1-positive cells were MM cells (data not shown). These findings are consistent with increased proliferation of MM cells in vivo triggered by pDCs. Similarly, we noted a marked increase in p-IκB, a decrease in ubiquitination, and enhanced factor VIII and VEGFR1 expression in bone sections from mice injected with pDCs plus INA-6 cells versus INA-6 MM cells alone (Figures 7F–7H). These in vivo data confirm our in vitro data and suggest that pDCs trigger activation of growth, survival, and angiogenic signaling pathways in MM cells.

We next utilized a subcutaneous model of human MM in SCID mice to further confirm pDC-induced MM cell growth. An early and rapid growth of tumor occurred within 12 days in mice receiving both pDCs and MM cells, whereas similar tumor growth was noted only at day 21 in mice injected with MM cells alone (Figure 7I). Immunostaining showed increased IL-3 and presence of pDCs (BDCA-2$^+$ cells) in tumor sections from mice receiving pDCs and MM cells versus MM cells alone (data not shown). Together, our findings from two distinct human MM xenograft models suggest that pDCs enhance MM cell growth in vivo.

CpG-Containing Oligodeoxynucleotides Restore MM Patient pDCs T Cell Response and Block MM Cell Growth

MM is characterized by immune dysfunction, and pDCs may contribute, at least in part, because MM patient BM-pDCs exhibit reduced ability to induce T cell proliferation (Figure 1B). The loss of immune functioning of tumor-infiltrating DCs has been linked to the immunosuppressive effects of the tumor-host microenvironment mediated via VEGF, IL-6, or MCSF in cancers (Zou, 2005), including MM (Hayashi et al., 2003). Prior studies showed that immune function of pDCs is mediated by production of type I IFNs (Siegal et al., 1999), which, in turn, is linked to expression of Toll-like receptor 7 (TLR7) and TLR9 (Gilliet et al., 2008; Krieg, 2007; Moseman et al., 2004; Vollmer, 2005). Other studies have targeted TLR-9 using immunostimulatory activities of CpG-containing oligodeoxynucleotides (CpG-ODNs) to activate pDCs. Indeed systemic lupus erythematous is linked to TLR-9-activated pDCs and IFN-α release (Barrat et al., 2005; Krieg, 2007; Liu et al., 2008; Vollmer, 2005). In light of these studies, we next examined whether treatment of MM patient BM-pDCs with CpG-ODNs alters their T cell stimulatory activity. Importantly, CpG-ODNs restore the ability of MM patient BM-pDCs to trigger both allogeneic and autologus T cell proliferation (Figures 8A and 8B). Furthermore, CpGs also enhanced IFN-α secretion from MM patient BM-pDCs (Figure 8C) and upregulated TLR9 expression in MM BM pDCs (Figure 8D).

Prior studies showed that pDCs activated via TLR ligation, CD40-L engagement, or HIV can modulate regulatory T cells (Tregs) (Gilliet and Liu, 2002; Manches et al., 2008; Moseman et al., 2004). Tregs are dysfunctional and decreased in number in MM (Prabhala et al., 2006). CD4+CD25+FOXP3-high Tregs can be expanded by mDCs in vitro and after injection of cytokine-matured DCs in MM patients (Banerjee et al., 2006). It is possible that activated pDCs may restore Treg homeostasis in MM; however, the functional significance of pDCs effect on Tregs within the human MM BM microenvironment, particularly the biologic sequelae in MM cells, remains to be examined.

We next asked whether CpG-ODNs affect pDC-induced MM cell growth. As shown in Figure 8E, CpGs inhibit patient-BM pDC-triggered DNA synthesis in MM.1S cells. CpGs also blocked pDC-induced growth of MM cells lines, as assessed by WST proliferation assays (Figure 8F). These data demonstrate that (1) activation of pDCs with CpGs both restores their ability to trigger T cell proliferation and reduces their MM cell growth promoting activity; and (2) MM cell interaction with pDCs does not require pDC activation. A recent study in the B16 mouse melanoma tumor model also showed that CpG-activated pDCs are capable of inducing a systemic antitumor immunity via activation of NK cells and T cells (Liu et al., 2008). It remains to be determined whether CpG-activated MM pDCs generate clinically significant effective antitumor immunity in MM.

In summary, we show the pathophysiologic role of pDCs in MM. Our findings demonstrate increased numbers and more frequent localization of pDCs in MM patient BM than normal BM. Both in vitro and in vivo models of human MM show that pDCs confer growth, survival, chemotaxis, and drug resistance in MM cells. Targeting Toll-like receptors with CpG-ODNs both improves immune function of pDCs and abrogates pDC-induced MM cell growth. Overall, our findings identify an integral role of pDCs in MM pathogenesis and provide the basis for targeting pDC-MM interactions with CpG-ODNs as a therapeutic strategy to improve patient outcome in MM.

EXPERIMENTAL PROCEDURES

Isolation, Phenotypic Analysis, and Quantification of pDCs

All studies involving human samples were performed under IRB-approved protocols at Dana-Farber Cancer Institute (Boston), Brigham and Womens Hospital (Boston), and Mayo Clinic (Rochester), through which informed consent was obtained and de-identified samples were utilized. pDCs were isolated by magnetically activated cell sorting using CD304 (BDCA-4/Neuropilin-1) microbeads kit (Miltenyi Biotec, Auburn, CA). MNCs from normal healthy donors and MM patients were isolated by Ficoll Hypaque density gradient centrifugation. Cells were then magnetically labeled with anti-BDCA-4 antibody coupled to colloidal paramagnetic microbeads and passed through a magnetic separation column twice (Miltenyi Biotec). The cells staining negative for lineage markers and CD11c were FACS sorted (Figure 1A). Polychromatic staining of cells with CD123 PE-Cy5, HLA-DR Pacific Blue, and BDCA-2 FITC confirmed the purity of pDCs (≥99%) (Dzionek et al., 2001): BDCA-4-positive pDCs derived in this way are lineage (CD3, CD14, CD20, CD11c-) negative, MHC II positive, and CD123/BDCA-2 positive. pDCs were quantified in total MNCs (2×10^6 cells) from PB or BM samples using FACS analysis (100,000 minimum events were gated) with BDCA-2 (CD303)-PE conjugated antibody (Mitenyi Biotec). For some experiments, pDCs were purified using negative depletion (Miltenyi Biotec) (99% BDCA^{2+} CD123+ cells by FACS). To obtain pDC-depleted fraction of MM BM cells, we utilized LD columns in combination with BDCA-4 Microbeads and MACS separator (Miltenyi Biotec). FACS analysis of pDC-depleted BM cell fraction showed low to undetectable BDCA-2-positive cells (3.8% pDCs before and <0.02% pDCs after depletion). Antibody details are in Supplemental Data. Flow cytometric analysis was performed on a Beckman Coulter FC 500, and the data were analyzed with CXP software (BD Biosciences, San Jose, CA).

Cell Growth, Viability, Survival, and Apoptosis Assays

Cells were cultured in complete medium (RPMI-1640 media supplemented with 10% FBS, 100 U/ml penicillin, 100 μg/ml streptomycin, and 2 mM L-glutamine). DNA synthesis was measured by (^{3}H)thymidine uptake (^{3}H-Tdr) (PerkinElmer, Boston, MA), as previously described (Chauhan et al., 2005). Fold change in DNA synthesis was calculated using following formula: ^{3}H-TdR uptake of cells in pDC-MM cultures minus ^{3}H-TdR uptake of pDCs alone divided by ^{3}H-TdR uptake of MM cells alone. Growth was also assessed by

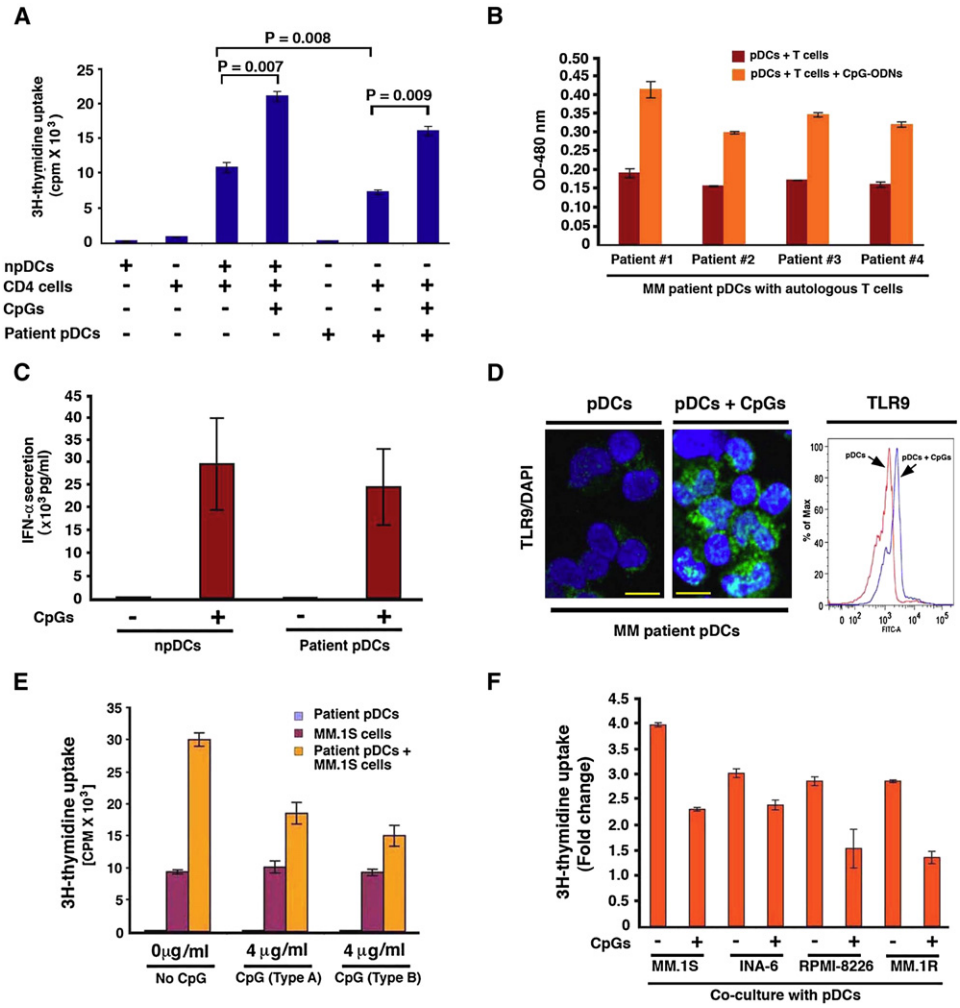

Figure 8. Therapeutic Implications of pDC-MM Cell Interactions

(A) Normal CD4 T cells (1×10^4) were cultured with normal pDCs or MM patient BM pDCs (1×10^5) (1:10 pDCs/T cells) in the presence or absence of CpGs for 5 days, and then analyzed for DNA synthesis (mean ± SD; n = 4).

(B) MM BM pDCs (1×10^4) were cultured with autologous T cells (1×10^5) (1:10 pDCs/T cells) in the presence or absence of CpGs (type A, 4 μg/ml) for 5 days and then analyzed for T cell proliferation with WST proliferation assay (mean ± SD; $p < 0.005$ for all patients).

(C) CpG-ODNs (type A, 4 μg/ml) restore IFN-α production from MM patient BM pDCs: Both normal PB pDCs and MM patient BM pDCs (10^5 cells) were cultured in the presence or absence of CpG-ODNs for 24 hr, and IFN-α levels were measured by ELISA (mean ± SD; $p = 0.01$, six MM patient BM pDCs and four normal pDCs were evaluated).

(D) pDCs were cultured in the presence or absence of CpG-ODNs for 12 hr; cytospins were prepared and subjected to immunostaining with anti-TLR9 antibody (green) and DAPI (blue). Representative micrographs from three experiments are shown. Scale bars represent 10 μM. Intracellular staining with TLR9 antibody followed by FACS analysis shows upregulation of TLR9 expression in CpG-treated MM pDCs.

(E) CpGs block MM BM pDC-induced MM.1S cell growth. pDCs, MM.1S cells, or pDCs + MM.1S cells (1:5 pDC/MM ratio) were cultured in the presence or absence of CpG-ODNs for 3 days, and DNA synthesis was measured with ^{3}H-TdR uptake (mean ± SD; $p < 0.004$, n = 4).

(F) MM cell lines were cultured with normal PB pDCs at 1:5 pDC/MM ratio in the presence or absence of CpGs for 3 days, and then analyzed for growth by WST proliferation assay (mean ± SD; $p < 0.005$, n = 4). Errors bars indicate SD.

WST assay (BioVision, Mountain View, CA). Cell viability was assessed by 3-(4,5-dimethylthiozol-2-yl)-2,5-diphenyltetrazolium bromide (MTT; Chemicon International Inc., Temecula, CA) assay (Chauhan et al., 2005). For cell survival assays, pDCs and patient MM cells were cultured at 1:5 pDC/MM ratio in six-well plates in DCP-MM culture medium (Mattek Corp. Ashland, MA). After each week of coculture, tumor cells were separated with CD138 microbeads, and cultured with fresh pDCs. After 4 weeks of coculture, cells were triple stained with CD138-FITC-conjugated antibody, CD123-PE-conjugated antibody, and DAPI, and images were taken by Zeiss LSM confocal microscope (Thornwood, NY). Staining with kappa and lambda antibodies and DAPI confirmed clonality of MM cells. Apoptosis was measured by Annexin V/PI staining (Chauhan et al., 2005). T cell proliferation assays were performed as previously described (Hayashi et al., 2003). Briefly, pDCs were cultured with or without T cells, in the presence or absence of CpG-ODNS (0.4 and 4.0 μg/ml) in complete medium; and DNA synthesis was analyzed by both ^{3}H-TdR uptake and WST assays.

Live-Cell Imaging

pDCs were labeled with MitoFluor Red 594 (1:1000; Invitrogen, Carlsbad, CA); GFP-positive MM.1S were added to pDCs in a 24 well glass-bottom culture

dish (MatTek Inc, Ashland, MA), and live-cell images were taken with an Apochromat 40×/1.2 W lens on a LSM-510 confocal system. Images were taken for 30 ms interval for 5–15 min, and processed using Volocity software (Improvision, Waltham, MA).

Immunofluorescence and Confocal Microscopy

BM biopsies from MM patients and normal donors were subjected to double IFC staining with BDCA-2 and CD138 antibodies. Antigen retrieval was performed by boiling the slides in DIVA Decloaker (Biocare, Concord CA) for 10 min in a pressure cooker. Slides were incubated with 5% normal donkey serum, followed by staining with mouse monoclonal anti-human CD138 antibody (1:100) and rabbit polyclonal BDCA-2 antibody (1:10). After Tris-buffered saline wash, slides were incubated with Alexa-488-conjugated donkey anti-rabbit secondary antibody (1:200) and CY5 donkey anti-mouse secondary antibody (1:200) for 1 hr at room temperature. Slides were mounted with Vectashield containing DAPI (Vector Laboratories, Burlingame CA). Confocal images were taken with the Zeiss LSM510 confocal system (63×/1.4 apochromat objective) (Thornwood, NY). IHC with primary antibody specific for pDCs (BDCA-2 at 1:400 dilution) and MM cells (CD138 at 1:500 dilution) was conducted in accordance with previously described methods (Jaye et al., 2006).

Transwell Migration Assays

In vitro migration assays were performed with Transwell Boyden chambers (Chemicon, Billerica, MA). For pDC chemotaxis studies, we utilized 5 μM pore size membranes, which allow for the free passage of pDCs. Afterward, 5×10^5 pDCs were suspended in serum-free culture medium (RPMI-1640 media supplemented with antibiotics) and plated in the upper chamber; the lower chamber was coated with various chemokines. After 2 hr incubation at 37°C, pDCs that migrated to the lower chamber were counted. pDC and MM cell migration was assayed with a 24-well plate with 8 μm pore size inserts. MM cells (2×10^6 cells/ml) were plated in the upper and pDCs in the lower chamber or vice versa. Serum-free culture medium (as above) was used. The plates were then incubated at 37°C for 4 hr, and the nonmigrating cells in the upper chamber removed from the Transwell membrane by washing with phosphate-buffered saline. Cells migrating to the bottom face of the membrane were stained with cresyl violet. Three randomly selected fields were examined to quantify number of cells migrating from upper to lower chambers. For cell-cell contact-dependent MM cell growth, we utilized two different pore-size membranes to separate cells: 0.4 μM (that does not allow free passage of cells) and 8 μM (that allows cell passage). pDCs (2×10^4) and MM.1S cells (1×10^5) were added into the upper and lower chamber, respectively, and incubated for 72 hr at 37°C; cells from the lower chamber were then harvested and analyzed for growth by WST assays.

Cytokine Bead Arrays and ELISA

MM.1S cells (5×10^4 cells/200 μl) and pDCs (1×10^4 cells/200 μl) were cultured either alone or together at 1:5 (pDC/MM) ratio in 96 well plates for indicated intervals in triplicate; supernatants were collected (a total of 600 μl for each condition) and analyzed with human cytokine/chemokine panel-29 Plex (Linco Diagnostic, St Charles, MO). Cells were cultured in complete medium. BAFF, SDF1-α, and IL-3 levels were measured by Quantikine BAFF ELISA kit (R&D Systems, Minneapolis, MN). IFN-α levels were assessed by ELISA (PBL, Piscataway, NJ).

Proteasome Activity Assays

MM.1S cells (2.5×10^6) and pDCs (0.5×10^6) were cultured in complete medium; MM.1S cells were separated from pDC cocultures by CD138 microbeads (purity > 99% $CD138^+$ cells), and proteasome activity assays were performed using fluorogenic peptide substrates, as previously described (Chauhan et al., 2005).

Human Plasmacytoma Xenograft and SCID-hu Model

All animal experiments were approved by and conform to the relevant regulatory standards of the Institutional Animal Care and Use Committee at the Dana-Farber Cancer Institute. SCID-hu model has been described previously (Tassone et al., 2005). For SCID-hu model studies, we utilized an IL-6-dependent INA-6 MM cell line. Cells were propagated in vitro in complete medium, and rhIL-6 (2.5 ng/ml). INA-6 cells (2×10^6) without IL-6, pDCs alone (0.4×10^6), or INA-6 cells together with pDCs were injected directly into human bone chips implanted subcutaneously in SCID mice. Tumor growth was assessed every tenth day by measuring circulating levels of shIL-6R and IgG levels in mouse blood using ELISA (R&D Systems). In the human plasmacytoma xenograft model, CB-17 SCID-mice were subcutaneously injected with pDCs alone, MM.1S cells alone, or pDCs and MM.1S cells (five mice per group) in plain RPMI-1640 medium, and tumor growth was measured as previously described (Chauhan et al., 2005).

Immunohistochemistry

Implanted human bone chips were excised from mice and subjected to IHC analysis with antibodies against Ki-67, cyclin-D1, p-IkB, factor VIII, VEGFR1, and ubiquitin (Abcam, Cambridge, MA), as previously described (Singh et al., 2006).

Statistical Analysis

Nonparametric tests and mixed models were used to analyze the data, including Wilcoxon's signed rank and/or Student's t test for proliferation assessment. Significance of differences observed in xenograft studies was assessed with the Student's t test. The minimal level of significance was $p < 0.05$.

ACCESSION NUMBERS

The raw data for expression profiling and the CEL files are can be found at the website Gene Expression Omnibus (http://www.ncbi.nlm.nih.gov/geo/) under accession number GSE17407.

SUPPLEMENTAL DATA

Supplemental Data include Supplemental Experimental Procedures, three figures, and a movie and can be found with this article online at http://www.cell.com/cancer-cell/supplemental/S1535-6108(09)00292-X.

ACKNOWLEDGMENTS

This investigation was supported by NIH grants SPORE-P50100707, PO1-CA078378, and RO1CA050947, and by Myeloma Research Foundation. D.C. designed research, analyzed data, and wrote the manuscript; A.S. designed, interpreted, and performed most experiments; M.B. performed growth/survival assays; G.B. isolated normal plasma cells; R.C. and D.J. helped with IHC; T.H., S.H., P.R., Y.T., N.R., C.M., and N.M. provided clinical samples; and K.A. analyzed data and wrote the manuscript. We also thank Robert Schlossman, Bryan Ciccarelli, and Sagar Lonial for providing blood samples. We are thankful to Lay-Hong Ang for confocal microscopy, John F. Daley for FACS, and Sangeetha Battar, Gaurav Chetri, and David Vasir for technical help and insightful discussions.

Received: March 26, 2008
Revised: March 12, 2009
Accepted: August 19, 2009
Published: October 5, 2009

REFERENCES

Anderson, K.C. (2007). Targeted therapy of multiple myeloma based upon tumor-microenvironmental interactions. Exp. Hematol. *35*, 155–162.

Banchereau, J., and Steinman, R.M. (1998). Dendritic cells and the control of immunity. Nature *392*, 245–252.

Banerjee, D.K., Dhodapkar, M.V., Matayeva, E., Steinman, R.M., and Dhodapkar, K.M. (2006). Expansion of FOXP3high regulatory T cells by human dendritic cells (DCs) in vitro and after injection of cytokine-matured DCs in myeloma patients. Blood *108*, 2655–2661.

Barrat, F.J., Meeker, T., Gregorio, J., Chan, J.H., Uematsu, S., Akira, S., Chang, B., Duramad, O., and Coffman, R.L. (2005). Nucleic acids of mammalian origin can act as endogenous ligands for Toll-like receptors and may promote systemic lupus erythematosus. J. Exp. Med. *202*, 1131–1139.

Bergsagel, P.L., and Kuehl, W.M. (2005). Molecular pathogenesis and a consequent classification of multiple myeloma. J. Clin. Oncol. *23*, 6333–6338.

Brenner, H., Gondos, A., and Pulte, D. (2008). Recent major improvement in long-term survival of younger patients with multiple myeloma. Blood *111*, 2521–2526.

Brimnes, M.K., Svane, I.M., and Johnsen, H.E. (2006). Impaired functionality and phenotypic profile of dendritic cells from patients with multiple myeloma. Clin. Exp. Immunol. *144*, 76–84.

Brown, R.D., Pope, B., Murray, A., Esdale, W., Sze, D.M., Gibson, J., Ho, P.J., Hart, D., and Joshua, D. (2001). Dendritic cells from patients with myeloma are numerically normal but functionally defective as they fail to up-regulate CD80 (B7-1) expression after huCD40LT stimulation because of inhibition by transforming growth factor-beta1 and interleukin-10. Blood *98*, 2992–2998.

Chauhan, D., Catley, L., Li, G., Podar, K., Hideshima, T., Velankar, M., Mitsiades, C., Mitsiades, N., Yasui, H., Letai, A., et al. (2005). A novel orally active proteasome inhibitor induces apoptosis in multiple myeloma cells with mechanisms distinct from Bortezomib. Cancer Cell *8*, 407–419.

Chauhan, D., Uchiyama, H., Akbarali, Y., Urashima, M., Yamamoto, K., Libermann, T.A., and Anderson, K.C. (1996). Multiple myeloma cell adhesion-induced interleukin-6 expression in bone marrow stromal cells involves activation of NF-kappa B. Blood *87*, 1104–1112.

Colonna, M., Trinchieri, G., and Liu, Y.J. (2004). Plasmacytoid dendritic cells in immunity. Nat. Immunol. *5*, 1219–1226.

Dalton, W., and Anderson, K.C. (2006). Synopsis of a roundtable on validating novel therapeutics for multiple myeloma. Clin. Cancer Res. *12*, 6603–6610.

Dzionek, A., Inagaki, Y., Okawa, K., Nagafune, J., Rock, J., Sohma, Y., Winkels, G., Zysk, M., Yamaguchi, Y., and Schmitz, J. (2002). Plasmacytoid dendritic cells: From specific surface markers to specific cellular functions. Hum. Immunol. *63*, 1133–1148.

Dzionek, A., Sohma, Y., Nagafune, J., Cella, M., Colonna, M., Facchetti, F., Gunther, G., Johnston, I., Lanzavecchia, A., Nagasaka, T., et al. (2001). BDCA-2, a novel plasmacytoid dendritic cell-specific type II C-type lectin, mediates antigen capture and is a potent inhibitor of interferon alpha/beta induction. J. Exp. Med. *194*, 1823–1834.

Garcia De Vinuesa, C., Gulbranson-Judge, A., Khan, M., O'Leary, P., Cascalho, M., Wabl, M., Klaus, G.G., Owen, M.J., and MacLennan, I.C. (1999). Dendritic cells associated with plasmablast survival. Eur. J. Immunol. *29*, 3712–3721.

Gilliet, M., Cao, W., and Liu, Y.J. (2008). Plasmacytoid dendritic cells: Sensing nucleic acids in viral infection and autoimmune diseases. Nat. Rev. Immunol. *8*, 594–606.

Gilliet, M., and Liu, Y.J. (2002). Generation of human CD8 T regulatory cells by CD40 ligand-activated plasmacytoid dendritic cells. J. Exp. Med. *195*, 695–704.

Grouard, G., Rissoan, M.C., Filgueira, L., Durand, I., Banchereau, J., and Liu, Y.J. (1997). The enigmatic plasmacytoid T cells develop into dendritic cells with interleukin (IL)-3 and CD40-ligand. J. Exp. Med. *185*, 1101–1111.

Hayashi, T., Hideshima, T., Akiyama, M., Raje, N., Richardson, P., Chauhan, D., and Anderson, K.C. (2003). Ex vivo induction of multiple myeloma-specific cytotoxic T lymphocytes. Blood *102*, 1435–1442.

Hideshima, T., Mitsiades, C., Tonon, G., Richardson, P.G., and Anderson, K.C. (2007). Understanding multiple myeloma pathogenesis in the bone marrow to identify new therapeutic targets. Nat. Rev. Cancer *7*, 585–598.

Jaye, D.L., Geigerman, C.M., Herling, M., Eastburn, K., Waller, E.K., and Jones, D. (2006). Expression of the plasmacytoid dendritic cell marker BDCA-2 supports a spectrum of maturation among CD4+ CD56+ hematodermic neoplasms. Mod. Pathol. *19*, 1555–1562.

Jego, G., Palucka, A.K., Blanck, J.P., Chalouni, C., Pascual, V., and Banchereau, J. (2003). Plasmacytoid dendritic cells induce plasma cell differentiation through type I interferon and interleukin 6. Immunity *19*, 225–234.

Krieg, A.M. (2007). TLR9 and DNA "feel" RAGE. Nat. Immunol. *8*, 475–477.

Kukreja, A., Hutchinson, A., Dhodapkar, K., Mazumder, A., Vesole, D., Angitapalli, R., Jagannath, S., and Dhodapkar, M.V. (2006). Enhancement of clonogenicity of human multiple myeloma by dendritic cells. J. Exp. Med. *203*, 1859–1865.

Kukreja, A., Hutchinson, A., Mazumder, A., Vesole, D., Angitapalli, R., Jagannath, S., O'Connor, O.A., and Dhodapkar, M.V. (2007). Bortezomib disrupts tumour-dendritic cell interactions in myeloma and lymphoma: Therapeutic implications. Br. J. Haematol. *136*, 106–110.

Kumar, S.K., Rajkumar, S.V., Dispenzieri, A., Lacy, M.Q., Hayman, S.R., Buadi, F.K., Zeldenrust, S.R., Dingli, D., Russell, S.J., Lust, J.A., et al. (2008). Improved survival in multiple myeloma and the impact of novel therapies. Blood *111*, 2516–2520.

Lee, J.W., Chung, H.Y., Ehrlich, L.A., Jelinek, D.F., Callander, N.S., Roodman, G.D., and Choi, S.J. (2004). IL-3 expression by myeloma cells increases both osteoclast formation and growth of myeloma cells. Blood *103*, 2308–2315.

Liu, C., Lou, Y., Lizee, G., Qin, H., Liu, S., Rabinovich, B., Kim, G.J., Wang, Y.H., Ye, Y., Sikora, A.G., et al. (2008). Plasmacytoid dendritic cells induce NK cell-dependent, tumor antigen-specific T cell cross-priming and tumor regression in mice. J. Clin. Invest. *118*, 1165–1175.

Liu, Y.J. (2005). IPC: Professional type 1 interferon-producing cells and plasmacytoid dendritic cell precursors. Annu. Rev. Immunol. *23*, 275–306.

MacLennan, I., and Vinuesa, C. (2002). Dendritic cells, BAFF, and APRIL: Innate players in adaptive antibody responses. Immunity *17*, 235–238.

Manches, O., Munn, D., Fallahi, A., Lifson, J., Chaperot, L., Plumas, J., and Bhardwaj, N. (2008). HIV-activated human plasmacytoid DCs induce Tregs through an indoleamine 2,3-dioxygenase-dependent mechanism. J. Clin. Invest. *118*, 3431–3439.

McKenna, K., Beignon, A.S., and Bhardwaj, N. (2005). Plasmacytoid dendritic cells: linking innate and adaptive immunity. J. Virol. *79*, 17–27.

Moseman, E.A., Liang, X., Dawson, A.J., Panoskaltsis-Mortari, A., Krieg, A.M., Liu, Y.J., Blazar, B.R., and Chen, W. (2004). Human plasmacytoid dendritic cells activated by CpG oligodeoxynucleotides induce the generation of CD4+CD25+ regulatory T cells. J. Immunol. *173*, 4433–4442.

Neri, P., Kumar, S., Fulciniti, M.T., Vallet, S., Chhetri, S., Mukherjee, S., Tai, Y., Chauhan, D., Tassone, P., Venuta, S., et al. (2007). Neutralizing B-cell activating factor antibody improves survival and inhibits osteoclastogenesis in a severe combined immunodeficient human multiple myeloma model. Clin. Cancer Res. *13*, 5903–5909.

O'Doherty, U., Peng, M., Gezelter, S., Swiggard, W.J., Betjes, M., Bhardwaj, N., and Steinman, R.M. (1994). Human blood contains two subsets of dendritic cells, one immunologically mature and the other immature. Immunology *82*, 487–493.

Oerlemans, R., Franke, N.E., Assaraf, Y.G., Cloos, J., van Zantwijk, I., Berkers, C.R., Scheffer, G.L., Debipersad, K., Vojtekova, K., Lemos, C., et al. (2008). Molecular basis of bortezomib resistance: proteasome subunit beta5 (PSMB5) gene mutation and overexpression of PSMB5 protein. Blood *112*, 2489–2499.

Poeck, H., Wagner, M., Battiany, J., Rothenfusser, S., Wellisch, D., Hornung, V., Jahrsdorfer, B., Giese, T., Endres, S., and Hartmann, G. (2004). Plasmacytoid dendritic cells, antigen, and CpG-C license human B cells for plasma cell differentiation and immunoglobulin production in the absence of T-cell help. Blood *103*, 3058–3064.

Prabhala, R.H., Neri, P., Bae, J.E., Tassone, P., Shammas, M.A., Allam, C.K., Daley, J.F., Chauhan, D., Blanchard, E., Thatte, H.S., et al. (2006). Dysfunctional T regulatory cells in multiple myeloma. Blood *107*, 301–304.

Ratta, M., Fagnoni, F., Curti, A., Vescovini, R., Sansoni, P., Oliviero, B., Fogli, M., Ferri, E., Della Cuna, G.R., Tura, S., et al. (2002). Dendritic cells are functionally defective in multiple myeloma: the role of interleukin-6. Blood *100*, 230–237.

Ribatti, D., Nico, B., and Vacca, A. (2006). Importance of the bone marrow microenvironment in inducing the angiogenic response in multiple myeloma. Oncogene *25*, 4257–4266.

Roodman, G.D. (2008). Novel targets for myeloma bone disease. Expert Opin. Ther. Targets *12*, 1377–1387.

Roodman, G.D., and Dougall, W.C. (2008). RANK ligand as a therapeutic target for bone metastases and multiple myeloma. Cancer Treat. Rev. *34*, 92–101.

Siegal, F.P., Kadowaki, N., Shodell, M., Fitzgerald-Bocarsly, P.A., Shah, K., Ho, S., Antonenko, S., and Liu, Y.J. (1999). The nature of the principal type 1 interferon-producing cells in human blood. Science *284*, 1835–1837.

Singh, A.V., Franke, A.A., Blackburn, G.L., and Zhou, J.R. (2006). Soy phytochemicals prevent orthotopic growth and metastasis of bladder cancer in mice by alterations of cancer cell proliferation and apoptosis and tumor angiogenesis. Cancer Res. *66*, 1851–1858.

Steinman, R.M., and Cohn, Z.A. (1973). Identification of a novel cell type in peripheral lymphoid organs of mice. I. Morphology, quantitation, tissue distribution. J. Exp. Med. *137*, 1142–1162.

Tabera, S., Perez-Simon, J.A., Diez-Campelo, M., Sanchez-Abarca, L.I., Blanco, B., Lopez, A., Benito, A., Ocio, E., Sanchez-Guijo, F.M., Canizo, C., and San Miguel, J.F. (2008). The effect of mesenchymal stem cells on the viability, proliferation and differentiation of B-lymphocytes. Haematologica *93*, 1301–1309.

Tassone, P., Neri, P., Carrasco, D.R., Burger, R., Goldmacher, V.S., Fram, R., Munshi, V., Shammas, M.A., Catley, L., Jacob, G.S., et al. (2005). A clinically relevant SCID-hu in vivo model of human multiple myeloma. Blood *106*, 713–716.

Vollmer, J. (2005). Progress in drug development of immunostimulatory CpG oligodeoxynucleotide ligands for TLR9. Expert Opin. Biol. Ther. *5*, 673–682.

Zou, W. (2005). Immunosuppressive networks in the tumour environment and their therapeutic relevance. Nat. Rev. Cancer *5*, 263–274.

Zou, W., Machelon, V., Coulomb-L'Hermin, A., Borvak, J., Nome, F., Isaeva, T., Wei, S., Krzysiek, R., Durand-Gasselin, I., Gordon, A., et al. (2001). Stromal-derived factor-1 in human tumors recruits and alters the function of plasmacytoid precursor dendritic cells. Nat. Med. *7*, 1339–1346.